Morphological instability of misfit-strained core-shell nanowires

V. Schmidt,[1,2,*] P. C. McIntyre,[1] and U. Gösele[2]
[1]*Department of Materials Science and Engineering, Stanford University, Stanford, California 94305, USA*
[2]*Max-Planck-Institut für Mikrostrukturphysik, Weinberg 2, D-06120 Halle, Germany*
(Received 7 February 2008; published 3 June 2008)

We investigate the morphological instability of a misfit-strained cylindrical core-shell nanowire by performing a linear stability analysis. For this aim, the stress and strain distributions of a core-shell nanowire with a sinusoidally perturbed surface are calculated to first order, properly accounting for the core-shell interface. In addition, the effect of surface stress on the stress and/or strain distributions is considered. Due to the large surface-to-volume ratio of nanosized objects, this is indispensable. The outcome of the stability analysis is threefold: First, our calculation shows that surface stress strongly influences the nature of the fastest growing mode of perturbation. It turns out that the axially symmetric mode does not necessarily grow fastest. Second, we find that the system is most unstable in the initial phase of shell growth, i.e., for thin shell thicknesses. Interestingly, considering thin shells and large misfits ($\gtrsim 3\%$), we find that there exists a core radius for which stability becomes maximal. Under the conditions considered this radius is in the range of about 5–10 nm. Third, there exists a parameter range for which the experimental observation that Ge-rich islands grown on thick silicon nanowires tend to be aligned in two rows on the opposite sides of the nanowire agrees with the outcome of our calculation.

DOI: 10.1103/PhysRevB.77.235302 PACS number(s): 68.65.−k, 81.10.Bk, 81.05.Cy

I. INTRODUCTION

Synthesizing epitaxial and dislocation free core-shell nanowires in which the shell material has a large lattice misfit with respect to the core is an experimentally challenging but scientifically rewarding task. Rewarding because one can in principle achieve very high stresses and strains in the nanowire core, which, considering Si-Ge-core-shell nanowires, for example, would cause strong changes in the band structure. From an electronic device point of view this is appealing because by straining the material one can increase the charge carrier mobility.[1] In case of a core-shell structure, this mobility increase could be further enhanced by a carefully chosen core-shell band alignment and doping profile.[2] Together with the possibility of realizing a surround-gate architecture,[3] this could be an interesting approach to high performance devices.

Yet, experimentally realizing a strongly strained core-shell structure is not trivial. This is because the system tends to relax the misfit strain by either developing a modulation of the surface, potentially leading to the creation of islands or notches on the surface, or by forming misfit dislocations. Tersoff and LeGoues[4] showed that the competition of these two relaxation mechanisms is such that for small lattice misfits the introduction of dislocations is favored, whereas large misfits promote the creation of islands or notches on the surface. The creation of islands or notches is usually related to the so-called Asaro–Tiller–Grinfel'd instability,[5,6] a strain induced morphological instability of the surface. Roughly speaking, one could describe the underlying mechanism by stating that for certain surface modulations, the energetic costs of increasing the surface area are smaller than the gain of reducing the elastic energy. Considering the growth of misfit-strained films on planar substrates, this instability has been the subject of extensive investigations.[7–10] However, these results may not be directly applicable to misfit-strained core-shell nanowires. Besides the pure geometrical differences, this is mainly caused by the fact that a bulk substrate is much less susceptible to the deformation by a strained layer than a nanowire. In case of a misfit-strained core-shell nanowire, one expects that a considerable part of the elastic energy is stored in the core, whereas in case of a bulk substrate the strained film basically contains the whole elastic energy. Another important difference between planar substrates and nanowires is that, due to their large surface-to-volume ratio, the morphological instability of core-shell nanowires critically depends on the surface stress.

In this work, we investigate the misfit driven morphological instability related to the creation of islands on the surface of core-shell nanowires by performing a linear stability analysis. We will use boundary conditions that are as realistic as possible, which means that we will properly account for the misfit at the interface, instead of just assuming a unidirectional stress along the centerline of the wire.[11,12] Furthermore, we will not limit ourselves to axially symmetric modulations of the surface.[12,13] Since the presence of islands usually breaks axial symmetry,[14] one has to take nonaxially symmetric modulations into account. Last, the effect of surface stress is properly accounted for.

II. THEORY

The system under consideration is a cylindrical core-shell nanowire with the shell grown epitaxially and dislocation free onto the core material. The shell material is assumed to possess a certain lattice misfit m with respect the core, so that both core and shell become elastically strained. For simplicity the mechanical constants, i.e., the shear modulus G, the Poisson ratio ν, the surface stress τ, and the surface free energy γ, are taken to be isotropic. Tensors and vectors are either indicated by Roman summation indices (adopting Einstein's summation convention) or by bold font symbols.

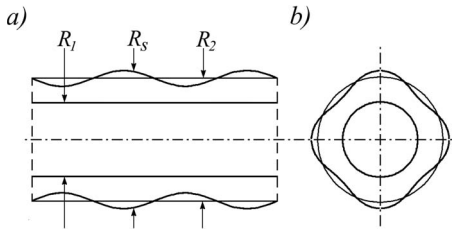

FIG. 1. Schematic of core-shell nanowire with a sinusoidal perturbation ($n=4, q\approx 2\pi/R_2$) of the surface; R_1 and R_2 are the initial core and shell radii, respectively and R_s is the surface radius. (a) Side view and (b) cross-sectional view.

The scheme of the linear stability analysis, following the works of Mullins[15] and Spencer *et al.*,[10] is simple. Core-shell nanowires are in reality not perfectly cylindrical. Instead, they show local deviations of cylindrical geometry. Thinking in Fourier space, these local deviations correspond to a broad distribution of sinusoidal surface modulations, which can be characterized by their wave number q in axial direction (the $\hat{\mathbf{z}}$ direction) and the mode number n in circumferential direction. Thus, if the outer radius of the unperturbed core-shell nanowire is R_2, and δ is the amplitude of the perturbation, then the actual surface radius R_s can be expressed as

$$R_s = R_2 + \delta\cos(qz)\cos(n\phi). \tag{1}$$

This is schematically depicted in Fig. 1 for a perturbation with $n=4$ and $q\approx 2\pi/R_2$. Of course, such modulations of the shell thickness also affect the stress and strain distributions within the nanowire and cause variations of the elastic energy. These variations can drive surface diffusion, and the question to be answered is whether surface diffusion ultimately leads to an increase or a decrease in the initial amplitude of modulation.

To answer this question the stress and strain distributions are calculated in a perturbative fashion. After some definitions, the zeroth order contributions, i.e., the stress and strain distribution of a cylindrical misfit-strained core-shell nanowire, are given in Sec. II A. All resulting zeroth order quantities such as the displacement $\bar{u}_i$, the strain $\bar{u}_{ij}$, the elastic strain $\bar{\epsilon}_{ij}$, or the stress $\bar{\sigma}_{ij}$ will be marked by an overbar. In Sec. II B we will then compute the changes to the stress and strain distribution to first order in δ, where all first order quantities will be marked by a tilde, symbolizing the waviness of the surface. Thus, we can write

$$u_i^\alpha = \bar{u}_i^\alpha + \tilde{u}_i^\alpha + \mathcal{O}(\delta^2), \tag{2}$$

$$u_{ij}^\alpha = \bar{u}_{ij}^\alpha + \tilde{u}_{ij}^\alpha + \mathcal{O}(\delta^2), \tag{3}$$

$$\epsilon_{ij}^\alpha = \bar{\epsilon}_{ij}^\alpha + \tilde{\epsilon}_{ij}^\alpha + \mathcal{O}(\delta^2), \tag{4}$$

$$\sigma_{ij}^\alpha = \bar{\sigma}_{ij}^\alpha + \tilde{\sigma}_{ij}^\alpha + \mathcal{O}(\delta^2). \tag{5}$$

The index α takes the values 1 or 2, where 1 stands for the nanowire core and 2 for the shell. Terms that are of second or higher order in δ will be neglected. To determine the zeroth and first order stress and strain distributions, we assume that the system is in equilibrium, so that in the absence of external body forces the displacement vector $\mathbf{u}$ has to fulfill the equations of equilibrium,[16]

$$(1-2\nu)\Delta\mathbf{u} + \nabla(\nabla\cdot\mathbf{u}) = 0. \tag{6}$$

Considering the symmetry of the problem one can solve the above equations. By additionally imposing proper boundary conditions one can then obtain explicit solutions for the displacement vector $\mathbf{u}$. Using cylindrical coordinates, i.e., $\mathbf{u} = u_r\hat{\mathbf{r}} + u_\phi\hat{\phi} + u_z\hat{\mathbf{z}}$, the components of the strain tensor u_{ij} are defined as[16]

$$u_{rr} = \partial_r u_r, \tag{7}$$

$$u_{zz} = \partial_z u_z, \tag{8}$$

$$u_{\phi\phi} = r^{-1}\partial_\phi u_\phi + r^{-1}u_r, \tag{9}$$

$$u_{rz} = (\partial_z u_r + \partial_r u_z)/2, \tag{10}$$

$$u_{\phi z} = (r^{-1}\partial_\phi u_z + \partial_z u_\phi)/2, \tag{11}$$

$$u_{r\phi} = (\partial_r u_\phi - r^{-1}u_\phi + r^{-1}\partial_\phi u_r)/2. \tag{12}$$

Completely analogous equations are valid for $\bar{u}_{ij}$ and $\tilde{u}_{ij}$. So we will use Eqs. (7)–(12) also for $\bar{u}_{ij}$ and $\tilde{u}_{ij}$ by imagining a bar or tilde set over each displacement or strain component. In Eq. (4) we introduced the elastic strain tensor ϵ_{ij}. This differentiation between u_{ij} and ϵ_{ij} is necessary to account for the lattice misfit at the core-shell interface. If the misfit parameter m is defined as

$$m = \frac{l_2 - l_1}{l_1}, \tag{13}$$

with l_1 and l_2 being the lattice constants of the core and the shell, respectively, one can implement the misfit strain by introducing the following relation between the strain tensor u_{ij} and the elastic strain tensor:

$$\epsilon_{ij}^\alpha = u_{ij}^\alpha - m\delta_{ij}\delta_{\alpha 2}. \tag{14}$$

Here both δ_{ij} and $\delta_{\alpha 2}$ denote a Kronecker delta. One can see that the elastic strain of the nanowire shell is "corrected" by the misfit strain. Moreover, the above definitions ensure that compressive stresses and/or strains are negative and tensile stresses and/or strains are positive. The stress tensor[16] is defined as

$$\sigma_{ij}^\alpha = \frac{2G_\alpha}{1-2\nu_\alpha}[(1-2\nu_\alpha)\epsilon_{ij}^\alpha + \nu_\alpha\epsilon_{ll}^\alpha\delta_{ij}], \tag{15}$$

with G_α and ν_α being the shear modulus and the Poisson ratio of the core or shell, respectively (α is not to be summed over). Together with Eq. (14) this leads to the following relation between σ_{ij} and u_{ij}:

$$\sigma_{ij}^\alpha = \frac{2G_\alpha}{1-2\nu_\alpha}[(1-2\nu_\alpha)u_{ij}^\alpha + \nu_\alpha u_{ll}^\alpha\delta_{ij} - (1+\nu_\alpha)m\delta_{ij}\delta_{\alpha 2}]. \tag{16}$$

These results can now be applied to the zeroth order quantities,

$$\bar{\epsilon}_{ij}^{\alpha} = \bar{u}_{ij}^{\alpha} - m\delta_{ij}\delta_{\alpha 2}, \tag{17}$$

$$\bar{\sigma}_{ij}^{\alpha} = \frac{2G_{\alpha}}{1-2\nu_{\alpha}}[(1-2\nu_{\alpha})\bar{u}_{ij}^{\alpha} + \nu_{\alpha}\bar{u}_{ll}^{\alpha}\delta_{ij} - (1+\nu_{\alpha})m\delta_{ij}\delta_{\alpha 2}], \tag{18}$$

and to the first order contributions,

$$\tilde{\epsilon}_{ij}^{\alpha} = \tilde{u}_{ij}^{\alpha}, \tag{19}$$

$$\tilde{\sigma}_{ij}^{\alpha} = \frac{2G_{\alpha}}{1-2\nu_{\alpha}}[(1-2\nu_{\alpha})\tilde{u}_{ij}^{\alpha} + \nu_{\alpha}\tilde{u}_{ll}^{\alpha}\delta_{ij}], \tag{20}$$

in accordance with Eqs. (3)–(5).

A. Zeroth order stress and strain

The first task is to find the stress and strain distributions of a cylindrical misfit-strained core-shell nanowire. The radial symmetry of the problem causes both the displacement $\bar{u}_{\phi}$ as well as the derivatives with respect to ϕ to be zero. Since the problem is taken to be translationally invariant with respect to translations in the $\hat{\mathbf{z}}$ direction and the end faces of the nanowire are assumed to be flat, $\partial_z\bar{u}_r = \partial_r\bar{u}_z = 0$. Under these conditions, the equations of equilibrium (6) can be reduced to the following two decoupled equations:

$$\partial_r^2\bar{u}_r^{\alpha} + \frac{1}{r}\partial_r\bar{u}_r^{\alpha} - \frac{1}{r^2}\bar{u}_r^{\alpha} = 0, \tag{21}$$

$$\partial_z^2\bar{u}_z^{\alpha} = 0, \tag{22}$$

having the solutions

$$\bar{u}_r^{\alpha} = a_{\alpha}r + b_{\alpha}\frac{1}{r}, \tag{23}$$

$$\bar{u}_z^{\alpha} = c_{\alpha}z, \tag{24}$$

with a_{α}, b_{α}, and c_{α} being six undetermined constants. One constant can directly be eliminated as $\bar{u}_r$ has to be finite at $r=0$, wherefore $b_1=0$. Thus, the problem is reduced to determining the five unknowns, a_1, a_2, b_2, c_1, and c_2, by imposing proper boundary conditions.

Before coming to the determination of these five unknowns, we would like to add some general remarks here on the role of the nanowire surface. As first recognized by Gibbs[17] and much later pointed out by Shuttleworth,[18] the surface free energy γ of a solid does not necessarily equal the surface stress τ. The surface free energy γ is related to the work of creating new area, e.g., by splitting, whereas the surface stress τ is related to the work of increasing the surface area by elastic deformation.[19] In principle, this work has to be characterized by introducing a second rank tensor τ_{ij}, the surface stress tensor. However, for isotropic surfaces this tensor $\tau_{ij}=\tau\delta_{ij}$ reduces to a scalar, the surface stress τ. This distinction between the surface free energy γ on the one hand and the surface stress τ on the other is important for this calculation, as we need γ to describe surface diffusion and τ for the boundary conditions of the strain problem.

In equilibrium the position of the boundary surface has to be stable, which is equivalent to stating that any net force in normal direction has to vanish. In case of a macroscopic solid-fluid interface this leads to

$$\sigma_{ij}n_j + P^f n_i = 0,$$

with n_j being the outward surface normal and P^f being the pressure in the surrounding fluid. Thus, a positive pressure P^f causes the normal component of the stress to be negative, i.e., compressive.

However, one has to be careful, as this condition, though customarily used in standard textbooks, implicitly neglects the surface stress contribution. Though being a reasonable approximation for macroscopic or even microscopic problems, this is not valid for nanoscopic problems with large surface-to-volume ratio. Considering nanoscopic problems with length scales on the order of τ/G, surface stress cannot be neglected, and one has to account for that in the boundary conditions.

Imagine a curved square-shaped surface element with the sides being parallel aligned with respect to the principle directions of curvature. Then a positive surface stress means that in-plane forces are pulling at the sides of the surface element. One can easily show using elementary geometry that this corresponds to a force equal to $-\tau\kappa n_i$, with κ being the sum of the principle curvatures and n_i being the outward surface normal. So the boundary conditions to be used at solid-fluid interfaces are

$$\sigma_{ij}n_j + P^f n_i + \tau\kappa n_i = 0. \tag{25}$$

A more rigorous derivation of the above equation is given in Eq. (B2).

In our case, we can neglect the pressure P^f. Under typical experimental conditions P^f is orders of magnitude smaller than the values of the bulk stress. Furthermore, we assume that, due to the epitaxial nature of the core-shell interface, the interface stress is small enough to be neglected. Thus, the conditions to be imposed are as follows.

(i) Equality of displacements at the core-shell interface. This ensures the epitaxial nature of the core-shell interface and leads to Eqs. (26) and (27).

(ii) Zero net normal force at the core-shell interface. Neglecting interface stress and using the outward normal $\bar{n}_i^{(1)}$ of the core-shell interface, this gives

$$\bar{\sigma}_{ij}^{(1)}\bar{n}_j^{(1)}\big|_{r=R_1} = \bar{\sigma}_{ij}^{(2)}\bar{n}_j^{(1)}\big|_{r=R_1}.$$

Using $\bar{n}_j^{(1)} = \hat{\mathbf{r}}$ leads to Eq. (28).

(iii) Zero net force in the $\hat{\mathbf{z}}$ direction. Considering that surface stress also creates a force in the $\hat{\mathbf{z}}$ direction leads to

$$\int_0^{R_1} \bar{\sigma}_{zz}^{(1)} 2\pi r dr + \int_{R_1}^{R_2} \bar{\sigma}_{zz}^{(2)} 2\pi r dr + \tau 2\pi R_2 = 0.$$

Since σ_{zz}^{α} has no r dependence, the integrals are trivial [see Eq. (29)].

(iv) Zero net normal force at the surface. As discussed,

$$\bar{\sigma}_{ij}^{(2)}\bar{n}_j^{(2)}|_{r=R_2} + \tau\frac{1}{R_2}\bar{n}_i^{(2)} = 0.$$

Together with $\bar{n}_j^{(2)} = \hat{\mathbf{r}}$, this gives Eq. (30).

So we end up with the following set of boundary conditions:

$$\bar{u}_r^{(1)}|_{R_1} = \bar{u}_r^{(2)}|_{R_1}, \tag{26}$$

$$\bar{u}_z^{(1)}|_{R_1} = \bar{u}_z^{(2)}|_{R_1}, \tag{27}$$

$$\bar{\sigma}_{rr}^{(1)}|_{R_1} = \bar{\sigma}_{rr}^{(2)}|_{R_1}, \tag{28}$$

$$R_1^2\bar{\sigma}_{zz}^{(1)} + (R_2^2 - R_1^2)\bar{\sigma}_{zz}^{(2)} = -2\tau R_2, \tag{29}$$

$$\bar{\sigma}_{rr}^{(2)}|_{R_2} = -\frac{\tau}{R_2}. \tag{30}$$

For simplicity we will from now on take $G_1 = G_2 = G$ and $\nu_1 = \nu_2 = \nu$. That is, we use the same material parameters for both core and shell, which is a reasonable approximation for many prominent material combinations such as Si-Ge, GaAs-AlAs, GaN-AlN, and others. Extending the model to nonidentical material constants is straightforward. Solving the boundary conditions [Eqs. (26)–(30)] for the five unknowns gives

$$a_1 = \frac{m(1-3\nu)(R_2^2 - R_1^2)}{2(1-\nu)R_2^2} - \frac{\tau(1-3\nu)}{2G(1+\nu)R_2}, \tag{31}$$

$$a_2 = \frac{m[2R_2^2(1-\nu) - R_1^2(1-3\nu)]}{2(1-\nu)R_2^2} - \frac{\tau(1-3\nu)}{2G(1+\nu)R_2}, \tag{32}$$

$$b_1 = 0, \tag{33}$$

$$b_2 = \frac{-m(1+\nu)R_1^2}{2(1-\nu)}, \tag{34}$$

$$c_1 = \frac{m(R_2^2 - R_1^2)}{R_2^2} - \frac{\tau(1-\nu)}{G(1+\nu)R_2}, \tag{35}$$

$$c_2 = c_1, \tag{36}$$

with these expressions used in Eqs. (23) and (24) one obtains the displacements $\bar{u}_r$ and $\bar{u}_z$, from which one can derive the strain tensor $\bar{u}_{ij}$ [using Eqs. (7)–(12)], the elastic strain tensor $\bar{\epsilon}_{ij}$ [using Eq. (17)], and the stress tensor $\bar{\sigma}_{ij}$ [using Eq. (18)].

Before we proceed with the calculation, we will examine the effect of surface stress τ on the elastic strain component,

$$\bar{\epsilon}_{zz} = \frac{m(\delta_{\alpha 1} - R_1^2)}{R_2^2} - \frac{\tau(1-\nu)}{2GR_2(1+\upsilon)}. \tag{37}$$

One can see that taking into account a positive surface stress (in contrast to the surface free energy γ, the surface stress of a solid can also be negative), the resulting $\bar{\epsilon}_{zz}$ is shifted by a negative term proportional to τR_2^{-1}, corresponding to an additional compressive force.

Consider, for example, a 7 nm diameter $Si_{0.8}Ge_{0.2}$ nanowire covered by a 3 nm Si shell, which corresponds to a misfit of $m = -0.0089$. To compute the elastic strain using Eq. (37) we need a reasonable estimate for the magnitude of τ, which turns out to be elusive, as the surface stress values of Si and Ge exhibit a pronounced anisotropy,[20–22] depend on the type of surface reconstruction,[23–26] and are additionally altered by the presence of adatoms.[27,28] For example, the surface stress values calculated by Meade and Vanderbilt[27] for a Si (111) surface range from −0.7 to 2.4 N/m depending on the specific surface configuration. In view of these ambiguities we will simply use a surface stress value of $\tau = 1$ N/m, which we think is a fair estimate considering the values given in Refs. 23–28.

Using $G = 46$ GPa and $\nu = 0.26$,[29] the strain ϵ_{zz} computes to −0.83% (−0.63%) in the nanowire core and 0.06% (+0.26%) in the shell, respectively. The numbers in parentheses give the corresponding values for $\tau = 0$. Thus, for this example, surface stress shifts the strain by −0.20%, leading to an increased strain in the core and an almost vanishing strain in the shell. This is really remarkable, as it means that one can in principle grow stress free shells on strained cores just by going to small enough radii. Furthermore, note that a nonzero surface stress necessarily breaks the antisymmetry of stress and strain with respect to sign changes in m. With surface stress considered, stress and strain are antisymmetric with respect to a simultaneous sign changes in both m and τ.

B. First order contribution to stress and strain

Next, we examine how adding a sinusoidal perturbation changes the stress and/or strain distribution. To arrive at expressions for the first order contributions, $\tilde{\epsilon}_{ij}$ or $\tilde{\sigma}_{ij}$ is in principle as straightforward as we have seen in Sec. II. However, instead of solving the equations of equilibrium (6) for the displacements, we will search for a solution in terms of the so-called Papkovich–Neuber potentials[30,31] $\boldsymbol{\Psi}$ and ξ, with $\boldsymbol{\Psi} = \Psi_r\hat{\mathbf{r}} + \Psi_\phi\hat{\boldsymbol{\phi}} + \Psi_z\hat{\mathbf{z}}$ being a vector and ξ being a scalar potential. From these, the displacements can then be derived by using the following relation:[32]

$$\mathbf{u} = 4(1-\nu)\boldsymbol{\Psi} - \nabla(\mathbf{R}\cdot\boldsymbol{\Psi} + \xi), \tag{38}$$

with $\mathbf{R} = r\hat{\mathbf{r}} + z\hat{\mathbf{z}}$. The main advantage of the Papkovic–Neuber potentials is that they simplify solving the equations of equilibrium (6), as these are fulfilled if both potentials separately satisfy Laplace's equation

$$\Delta\cdot\boldsymbol{\Psi} = 0, \tag{39}$$

$$\Delta\xi = 0. \tag{40}$$

For a radially symmetric problem the solutions are

$$\xi^\alpha = [d_\alpha\mathcal{I}_n(qr) + e_\alpha\mathcal{K}_n(qr)]\cos(qz)\cos(n\phi), \tag{41}$$

$$\psi_r^\alpha = [f_\alpha\mathcal{I}_{n+1}(qr) + g_\alpha\mathcal{I}_{n-1}(qr) + h_\alpha\mathcal{K}_{n+1}(qr) + i_\alpha\mathcal{K}_{n-1}(qr)]\cos(qz)\cos(n\phi), \tag{42}$$

$$\psi_\phi^\alpha = [f_\alpha \mathcal{I}_{n+1}(qr) - g_\alpha \mathcal{I}_{n-1}(qr) + h_\alpha \mathcal{K}_{n+1}(qr) - i_\alpha \mathcal{K}_{n-1}(qr)\cos(qz)\sin(n\phi)], \quad (43)$$

$$\psi_z^\alpha = [j_\alpha \mathcal{I}_n(qr) + k_\alpha \mathcal{K}_n(qr)]\cos(qz)\cos(n\phi), \quad (44)$$

where $\mathcal{I}_n(qr)$ and $\mathcal{K}_n(qr)$ denote the modified Bessel functions of order n. Again, the task is to determine the values of the constants d_α, e_α, f_α, g_α, h_α, i_α, j_α, and k_α. Fortunately, one can greatly reduce the number of unknowns by taking both the symmetry and the finiteness of the solution into account.

Consider the diagonal strain component in the $\hat{\mathbf{z}}$ direction, which according to Eqs. (38) and (8) is given by

$$u_{zz} = (3-4\nu)\partial_z \Psi_z - r\partial_z^2 \Psi_r - \partial_z^2 \xi - \partial_z \Psi_z - z\partial_z^2 \Psi_z. \quad (45)$$

This strain component must exhibit the same periodicity as the perturbation. However, due to the last term in Eq. (45), this is only possible if $\psi_z = 0$ or equivalently if $j_\alpha = k_\alpha = 0$. So Eq. (38) simplifies to

$$\tilde{u}_r = 4(1-\nu)\psi_r - \partial_r(r\psi_r^\alpha + \xi^\alpha), \quad (46)$$

$$\tilde{u}_z = -\partial_z(r\psi_r^\alpha + \xi^\alpha), \quad (47)$$

$$\tilde{u}_\phi = 4(1-\nu)\psi_\phi - r^{-1}\partial_\phi(r\psi_r^\alpha + \xi^\alpha). \quad (48)$$

One is tempted now to directly use Eqs. (41)–(44) and (46)–(48) in Eqs. (7)–(12) to derive expressions for the strains to be used in the boundary conditions. Yet, one has to be careful here, as this is only correct for modes with $n \neq 1$.

The problem with the $n=1$ mode arises when one tries to directly derive the strain using Eqs. (7)–(12). Due to the r^{-1} terms in Eqs. (9), (11), and (12), these expressions would give infinite strains unless the displacements $\tilde{u}_r$ and $\tilde{u}_\phi$ [see Eqs. (49) and (50)] are zero to at $r=0$.

$$\tilde{u}_r|_{r=0} = \left((3-4\nu)g_1 - \frac{q}{2}d_1\right)\delta_{n1}\cos(qz)\cos(n\phi), \quad (49)$$

$$\tilde{u}_\phi|_{r-0} = \left((3-4\nu)g_1 - \frac{q}{2}d_1\right)\delta_{n1}\cos(qz)\sin(n\phi). \quad (50)$$

Note that due to δ_{n1} in Eqs. (49) and (50), the displacements $\tilde{u}_r$ and $\tilde{u}_\phi$ at $r=0$ are nonzero only in case of the $n=1$ mode. In order to eliminate this potential divergence of the strain, we have to subtract expressions (49), Eq. (49) from Eq. (46), and Eq. (48) before applying Eqs. (7)–(12).

Why we only obtain nonzero displacements at $r=0$ in case of the $n=1$ mode can be seen in Fig. 2, which shows a schematic of the first three modes, $n=0$, $n=1$, and $n=2$. Due to symmetry reason, the radially symmetric $n=0$ pertubation cannot effect any nonzero displacements $\tilde{u}_r$ and $\tilde{u}_\phi$ at $r=0$, i.e., at the center of symmetry center. Also in case of the $n=2$ mode, which shows a twofold symmetry, the effects of the perturbation will cancel out at $r=0$. Only in case of the $n=1$ mode, where you have one bump on one side and a recess on the opposite side of the wire $\tilde{u}_r$ and $\tilde{u}_\phi$ can become

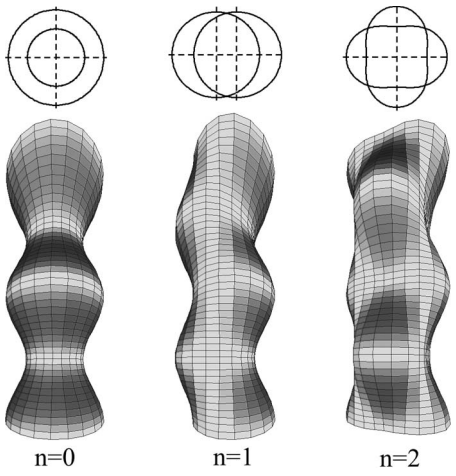

FIG. 2. Schematic cross section and 3D view of the three first modes $n=0$, $n=1$, and $n=2$; the amplitude of the perturbation was chosen to be $R_2/4$. Only in case of the $n=1$ mode the center of the cross section shifts with z.

nonzero at $r=0$. One can interpret this nonzero displacement as a bending of the wire as a whole, resulting in case of the $n=1$ mode in a slight S shape.

Let us come back now to determining the unknowns in general solutions (41)–(44). We can eliminate three constants by demanding that the solution has to be finite at $r=0$, wherefore e_1, h_1, and i_1 are bound to be zero. The remaining nine constants we have to determine with the help of an equal number of boundary conditions. For this aim it is useful to introduce the normal vectors $\tilde{n}_i^{(1)}$ and $\tilde{n}_i^{(2)}$ of the core-shell interface and of the surface, respectively. Since the core is assumed to be cylindrical, $\tilde{\mathbf{n}}^{(1)} = \hat{\mathbf{r}}$. Neglecting the second order terms, the surface normal $\tilde{\mathbf{n}}^{(2)} = \hat{\mathbf{r}} + \eta_\phi \hat{\phi} + \eta_z \hat{\mathbf{z}}$ with

$$\eta_\phi = \delta\frac{n}{R_2}\cos(qz)\sin(n\phi), \quad (51)$$

$$\eta_z = \delta q \sin(qz)\cos(n\phi), \quad (52)$$

and the curvature κ of the nanowire surface [see Eq. (A10)] is given by

$$\kappa = \frac{1}{R_2} + \delta\left(\frac{n^2-1}{R_2^2} + q^2\right)\cos(qz)\cos(n\phi). \quad (53)$$

The boundary conditions are as follows.

(i) Equality of displacements at the core-shell interface, leading to Eqs. (54)–(56).

(ii) Zero net normal force at the core-shell interface,

$$\sigma_{ij}^{(1)}\tilde{n}_j^{(1)}|_{r=R_1} = \sigma_{ij}^{(2)}\tilde{n}_j^{(1)}|_{r=R_1},$$

which by using $\sigma_{ij} = \bar{\sigma}_{ij} + \tilde{\sigma}_{ij}$ together with Eq. (28) and the fact that the interface normal $\tilde{\mathbf{n}}_j^{(1)} = \hat{\mathbf{r}}$ gives

$$\tilde{\sigma}_{ir}^{(1)}|_{r=R_1} = \tilde{\sigma}_{ir}^{(2)}|_{r=R_1}.$$

Since the shear components $\tilde{\sigma}_{\phi r}$ and $\tilde{\sigma}_{zr}$ are nonzero, this gives three conditions [see Eqs. (57)–(59)].

(iii) Zero net normal force at the surface,

$$\sigma_{ij}^{(2)}\tilde{n}_j^{(2)}|_{r=R_2} = -\bar{n}_i^{(2)}\tau\kappa.$$

Using Eq. (5) together with Eq. (28) gives

$$\tilde{\sigma}_{rr}^{(2)}|_{r=R_2} - \tau\frac{1}{R_2} = -\tau\kappa,$$

$$\tilde{\sigma}_{\phi r}^{(2)}|_{r=R_2} + \eta_\phi\bar{\sigma}_{\phi\phi}^{(2)}|_{r=R_2} = -\eta_\phi\tau\kappa,$$

$$\tilde{\sigma}_{zr}^{(2)}|_{r=R_2} + \eta_z\bar{\sigma}_{zz}^{(2)}|_{r=R_2} = -\eta_z\tau\kappa.$$

Inserting Eqs. (51)–(53) and eliminating second order terms then result in Eqs. (60)–(62). So finally we end up with the following boundary conditions:

$$\tilde{u}_r^{(1)}|_{R_1} = \tilde{u}_r^{(2)}|_{R_1}, \tag{54}$$

$$\tilde{u}_z^{(1)}|_{R_1} = \tilde{u}_z^{(2)}|_{R_1}, \tag{55}$$

$$\tilde{u}_\phi^{(1)}|_{R_1} = \tilde{u}_\phi^{(2)}|_{R_1}, \tag{56}$$

$$\tilde{\sigma}_{rr}^{(1)}|_{R_1} = \tilde{\sigma}_{rr}^{(2)}|_{R_1}, \tag{57}$$

$$\tilde{\sigma}_{r\phi}^{(1)}|_{R_1} = \tilde{\sigma}_{r\phi}^{(2)}|_{R_1}, \tag{58}$$

$$\tilde{\sigma}_{rz}^{(1)}|_{R_1} = \tilde{\sigma}_{rz}^{(2)}|_{R_1}, \tag{59}$$

$$\tilde{\sigma}_{rr}^{(2)}|_{R_2} = -\delta\tau\left(q^2 + \frac{n^2-1}{R_2}\right)\cos(qz)\cos(n\phi), \tag{60}$$

$$\tilde{\sigma}_{r\phi}^{(2)}|_{R_2} = -\delta\frac{n}{R_2}\left(\bar{\sigma}_{\phi\phi}^{(2)}|_{R_2} + \frac{\tau}{R_2}\right)\cos(qz)\sin(n\phi), \tag{61}$$

$$\tilde{\sigma}_{zr}^{(2)}|_{R_2} = -\delta q\left(\bar{\sigma}_{zz}^{(2)}|_{R_2} + \frac{\tau}{R_2}\right)\sin(qz)\cos(n\phi). \tag{62}$$

This set of equations has now to be solved for the nine unknown constants. However, one can show that for $G_1=G_2=G$ and $\upsilon_1=\upsilon_2=G$, Eqs. (54)–(59) are fulfilled if $e_2=h_2=i_2=0$, $d_1=d_2$, $f_1=f_2$, and $g_1=g_2$. Thus, it boils down to determining the values of d_2, g_2, and h_2 by solving Eqs. (60)–(62). Unfortunately, the solutions are still too long to be displayed. Instead the explicit forms of Eqs. (60)–(62) are given in Eqs. (B3)–(B5). With the expressions for d_2, g_2, and h_2 at hand, one can derive the displacements [using Eqs. (46)–(50)], the strain [using Eqs. (7)–(12)], the elastic strain [using Eq. (19)], and the stress [using Eq. (20)]. These results can then be combined with the corresponding zeroth order results to obtain the full stress and strain distributions to first order in δ.

One example of such a first order result is displayed in Fig. 3(b), which shows the elastic strain component $\epsilon_{zz}=\bar{\epsilon}_{zz}+\tilde{\epsilon}_{zz}$ as a function of r and z for a Ge-core (diameter of 15 nm) Si-shell (thickness of 5 nm) nanowire with an cosinusoidal perturbation ($n=0, q=2\pi/25$ nm^{-1}). The other parameters used are given in Fig. 3.

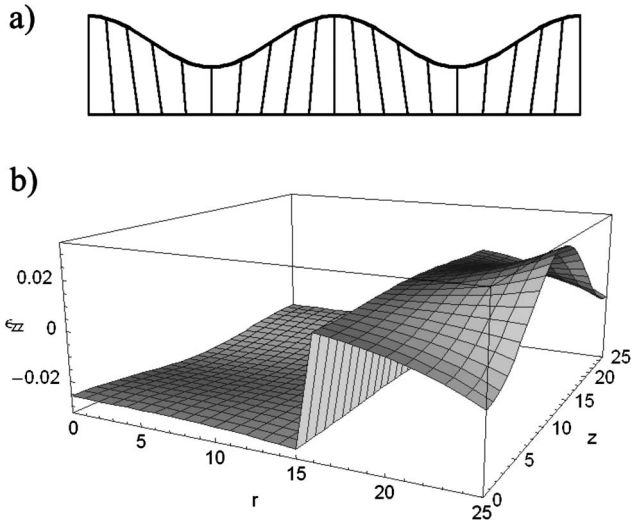

FIG. 3. (a) Schematic of a perturbed layer under tensile strain. (b) ϵ_{zz} as a function of r and z. $R_s=R_2+\delta\cos(qz)$, with $R_2=12.5$ nm and $q=\pi/R_2$. $R_1=7.5$ nm, $\delta=2$, $G=46$ GPa, $\nu=0.26$, $n=0$, $m=-0.043$, and $\tau=1.5$ N m^{-1}.

One can see in Fig. 3(b) that the core is compressively strained, whereas the shell is under tensile strain, as expected for a Ge-core-Si-shell structure. At the surface of the nanowire, the strain is reduced in the region where the shell is relatively thick (around $z=0$ and $z=\lambda=25$ nm). In the region around $z=\lambda/2$, where the shell thickness becomes minimal, the strain is considerably increased. This behavior can be intuitively understood by taking into account the schematic drawing shown in Fig. 3(a). In the regions where the shell is thicker than average, the strain is partly reduced by an elastic contraction of the shell. The contrary occurs in the regions where the shell is thinner than average. Here one would expect an increase in the tensile strain.

C. Linear stability analysis

According to Spencer *et al.*[9] the diffusion induced surface flux J_s can be expressed as[33–35]

$$J_s = \frac{-D_s\Gamma}{kT}\nabla_s M_\upsilon, \tag{63}$$

with D_s, Γ, and ∇_s being the surface diffusion constant, the area density of lattice sites, and the surface gradient, respectively; kT has its usual meaning. M_υ denotes the diffusion potential[9]

$$M_\upsilon = \Omega\left(\gamma'\kappa' + \frac{1}{2}\sigma_{ij}\epsilon_{ij}\right)_{r=R_s}, \tag{64}$$

with γ' and κ' being the surface energy density and the curvature of the (unstrained) reference state and Ω being the volume per atom. The diffusion potential has to be evaluated at the surface of the nanowire. Following the suggestion by Spencer *et al.*[9] we will neglect the difference between the actual state and the reference state and take the corresponding quantities γ and κ of the strained state instead. The 1/2

$\sigma_{ij}\epsilon_{ij}$ term is the energy density of the stress and/or strain field.

In addition to surface diffusion, we also consider the deposition of atoms onto the nanowire surface, going on at a rate Q, defined as the numbers of atoms per unit area and unit time. By employing the continuity equation, one can show that a radial vector $\mathbf{R_s}$ to a position on the surface will change with time as

$$\dot{\mathbf{R}}_\mathbf{s} = \Omega Q \tilde{\mathbf{n}}^{(2)} - \Omega(\nabla_s J_s)\tilde{\mathbf{n}}^{(2)}, \tag{65}$$

with the surface normal $\tilde{\mathbf{n}}^{(2)}$ defined in Eq. (A5). Inserting Eq. (63), the radial component of this vector equation becomes, to first order in δ, equal to

$$\dot{R}_s = \Omega Q + \frac{D_s \Gamma \Omega^2}{kT} \Delta_s \left(\gamma\kappa + \frac{1}{2}\sigma_{ij}\epsilon_{ij} \right)_{r=R_s}, \tag{66}$$

with Δ_s being the surface Laplace operator, whose first order expression is given in Eq. (A8). Using $\sigma_{ij}=\bar{\sigma}_{ij}+\tilde{\sigma}_{ij}$ and $\epsilon_{ij}=\bar{\epsilon}_{ij}+\tilde{\epsilon}_{ij}$ in the above equation and expanding the product would give four terms. Yet, the $\bar{\sigma}_{ij}\bar{\epsilon}_{ij}$ term is independent of z and ϕ and can therefore be omitted. Also the $\tilde{\sigma}_{ij}\tilde{\epsilon}_{ij}$ can be neglected, since it is of second order in δ, and the other two terms can be combined by using $\tilde{\sigma}_{ij}\bar{\epsilon}_{ij}=\bar{\sigma}_{ij}\tilde{\epsilon}_{ij}$. That this equality holds can be shown in a straightforward calculation by inserting Eqs. (17)–(20) and simplifying the expressions. Since all terms in parentheses in Eq. (66) are at least of order δ, it is sufficient to use the zeroth order approximation for the Laplacian Δ_s [see Eq. (A8)],

$$\Delta_s^0 = \frac{1}{R_2^2}\partial_\phi^2 + \partial_z^2. \tag{67}$$

Since we are only interested in first order contributions, we can evaluate the expression in parentheses at R_2 instead of R_s,

$$\dot{R}_s = \Omega Q + \frac{D_s \Gamma \Omega^2}{kT} \Delta_s^0 (\gamma\kappa + \bar{\sigma}_{ij}\tilde{\epsilon}_{ij})_{r=R_2}. \tag{68}$$

Due to the linear approximation, $\tilde{\epsilon}_{ij}$ must be proportional to δ. In addition, one can show using Eqs. (46)–(48) and (14) that $\tilde{\epsilon}_{ij}$ is proportional to $\cos(qz)\cos(n\phi)$, so that we can define a quantity $\tilde{\varepsilon}_{ij}$ that is independent of z and ϕ as

$$\tilde{\epsilon}_{ij} = \tilde{\varepsilon}_{ij}\delta\cos(qz)\cos(n\phi). \tag{69}$$

We can now insert the explicit forms of R_s and κ and perform Δ_s^0,

$$\dot{R}_2 + \dot{\delta}\cos(qz)\cos(n\phi) = \Omega Q + \frac{D_s \Gamma \Omega^2 \gamma}{kT}\left(\frac{n^2}{R_2^2} + q^2\right)\left(\frac{n^2-1}{R_2^2} + q^2 + \frac{\bar{\sigma}_{ij}\tilde{\varepsilon}_{ij}}{\gamma}\right)\delta\cos(qz)\cos(n\phi). \tag{70}$$

Separating the terms that are proportional to the cosines from those that are not then gives

$$\dot{R}_2 = \Omega Q, \tag{71}$$

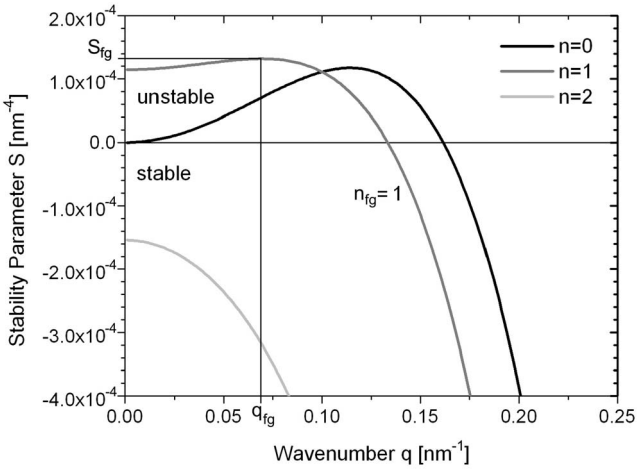

FIG. 4. Stability parameter S as a function of the wave number q for $R_1=7$ nm, $R_2=10$ nm, $G=46$ GPa, $\nu=0.26$, $m=-0.043$, $\tau=1.0$ N m^{-1}, and $\gamma=1.5$ J m^{-2}.

$$\dot{\delta} = \frac{D_s \Gamma \Omega^2 \gamma}{kT} S\delta, \tag{72}$$

with the stability parameter

$$S = \left(\frac{n^2}{R_2^2} + q^2\right)\left(\frac{1-n^2}{R_2^2} - q^2 - \frac{\bar{\sigma}_{ij}\tilde{\varepsilon}_{ij}}{\gamma}\right). \tag{73}$$

One can see that a uniform deposition on the surface, characterized by the parameter Q, causes an increase in the outer radius R_2. This change in R_2 would in principle also affect the magnitude of stability parameter S. However, if you assume that the radius change caused by the deposition happens on a much longer time scale, i.e., considering low deposition rates, you can decouple Eqs. (71) and (72) and consider the growth of the instability separately. In this case, the solution becomes

$$\delta(t) = \delta_0 \exp\left(\frac{D_s \Gamma \Omega^2 \gamma}{kT} St\right), \tag{74}$$

with δ_0 being the amplitude of the perturbation at $t=0$. This simple exponential time dependence corresponds to an increase in δ if $S>0$. That is the surface is unstable with respect to this particular perturbation. For $S<0$ the initial amplitude of perturbation decays exponentially with time, i.e., the cylindrical surface is stable with respect to this particular perturbation.

III. RESULTS AND DISCUSSION

We have seen that the time development of δ critically depends on the sign of the stability parameter S. Considering Eq. (73) it becomes clear that, were it is not for the $\bar{\sigma}_{ij}\tilde{\varepsilon}_{ij}$ term, larger values of q and n would lead to a smaller positive or larger negative value of S; that is, the shorter the wavelength of the perturbation, the more stable the surface. To give an impression of how the q dependence typically behaves, Fig. 4 shows S as a function of q for the first three modes for a 7 nm radius Ge nanowire covered by a 3 nm

thick Si shell. The surface free energy is taken to be $\gamma = 1.5$ J m^{-2}.[36,37]

First, one can see in Fig. 4 that the stability parameter S of the $n=0$ mode becomes zero in the limit $q \to 0$, exhibits a maximum, and becomes negative for large values of q. This behavior is very similar to what has been found by Spencer *et al.*[10] considering semi-infinite substrates. Thus, for this mode and wave numbers $q < 0.17$ nm^{-1} the amplitude of the perturbation would grow exponentially, corresponding to a roughening of the surface. Besides, we mention that for the $n=0$ mode, positive values of S can be found even for vanishing m, i.e., vanishing strain. In this case the maximum of S is located at about $2\pi\sqrt{2}R_2$, which corresponds to the wavelength of the classical Plateau-Rayleigh instability.[38,39]

Returning to Fig. 4, the $n=1$ mode exhibits a positive nonzero y-axis intercept and it can easily be derived that for $n=1$,

$$\lim_{q \to 0} S = \frac{2mR_1^2(1+\nu)[R_2\tau(1-2\nu) + 2GmR_1^2(1+\nu)]}{\gamma R_2^7(1-\nu)}. \tag{75}$$

One can see that for $\nu < 0.5$ and positive surface stress τ, the y-axis intercept of the $n=1$ mode is always positive. The $n=2$ mode on the other hand is negative for all wave numbers q. Thus, for the parameters chosen, only the $n=0$ and $n=1$ modes can cause a roughening of the surface and only for sufficiently long wavelengths.

Due to the exponential time dependence of Eq. (74), the perturbation having the largest values of S will grow the fastest. We will characterize this fastest growing mode by its values S_{fg}, q_{fg}, and n_{fg}. In Fig. 4 the fastest growing mode has $n_{fg}=1$ and $q_{fg} \approx 0.7$ nm^{-1}. In the following discussion we will mainly concentrate on the properties of the fastest growing modes and in particular on the dependencies of S_{fg} and n_{fg} on different parameters.

We first examine the properties of n_{fg}. In Fig. 5 n_{fg} is shown as a function of the core radius R_1 and the shell thickness $R_2 - R_1$ assuming a positive surface stress of $\tau = 1.0$ N m^{-1}. The misfit parameter is taken to be $m=-0.044$, which approximately corresponds to the misfit of a Si shell grown on a Ge core. One can see in Fig. 5 that for smaller shell thicknesses and/or larger radii, n_{fg} becomes larger and larger. However, most interesting is the comparison to the results for $m=+0.044$, which are not shown here, for they are too simple. For $m=+0.044$ and thickness and radius variations as shown in Fig. 5, the fastest growing mode always has $n_{fg}=0$. This difference in the nature of the fastest growing mode between $m=+0.044$ and $m=-0.044$ is a consequence of surface stress and can be understood by considering the $-\bar{\sigma}_{ij}\tilde{\varepsilon}_{ij}$ term in Eq. (73). Due to the boundary conditions at the nanowire surface, surface stress creates an additional compressive strain in the regions of positive curvature. Thus, in addition to the misfit induced strain, $\tilde{\varepsilon}_{ij}$ will also contain terms that are proportional to the product of the surface stress τ with curvature κ. The multiplication with $-\bar{\sigma}_{ij}$ will then create terms that are proportional to $-m\tau\kappa$. This contribution to S can either be positive or negative, depending on the sign of $m\tau$. So for positive τ and negative

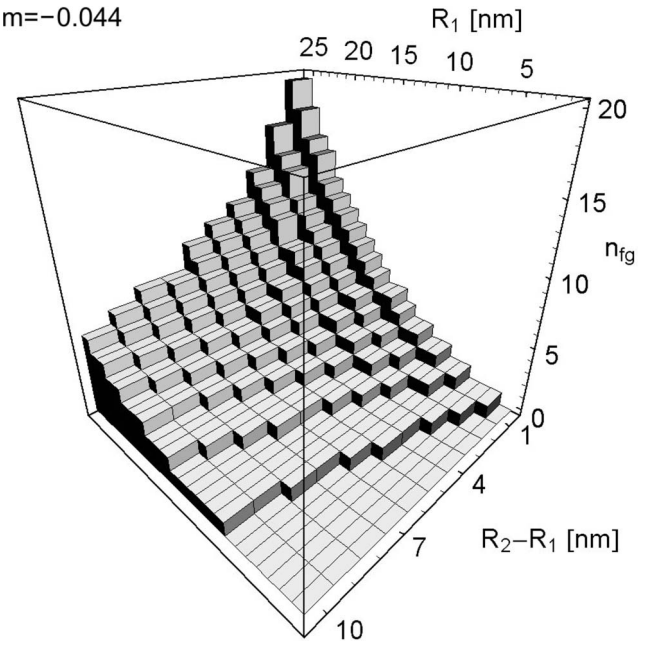

FIG. 5. n_{fg} as a function of the core radius R_1 and the shell thickness $(R_2 - R_1)$ for $m=-0.044$ using $G=46$ GPa, $\nu=0.26$, $\tau = 1.0$ N m^{-1}, and $\gamma=1.5$ J m^{-2}.

m, as shown in Fig. 5, this contribution will increase the value of S for those modes that have a large surface curvature, i.e., a large n. This means that including the contribution of a positive surface stress has the effect of increasing the growth rate of modes with large n. The opposite is true for positive m and positive τ, in which case surface stress stabilizes the surface with respect to the large n modes; with the result that the $n=0$ mode becomes the fastest growing mode.

We now focus on the stability parameter of the fastest growing mode. Figure 6 shows the decadic logarithm of S_{fg} as a function of core radius and shell thickness for $m = \pm 0.044$ assuming a positive surface stress of $\tau = 1.0$ N m^{-1}. The $m=+0.044$ and $m=-0.044$ cases, shown in Fig. 6, approximately correspond to Si-core-Ge-shell and Ge-core-Si-shell structures, respectively. The first feature that becomes immediately apparent is the strong dependence on the shell thickness. In both cases, $m=+0.044$ and $m=-0.044$, an increase in the shell thickness from 1 to 5 nm leads to a decrease in S_{fg} by at least 1 order of magnitude. Thus, concerning the overall stability one has to conclude that the initial phase of growth, where the shell is thinnest, is most critical with regards to a roughening of the surface. For experimentalists, this could signify that first growing an amorphous shell and then recrystallizing it in a second step might actually be the more promising approach because in this way one could possibly circumvent the instability problems occurring at very small shell thicknesses. The most interesting result, however, is the pronounced minimum one can find in Fig. 6(b) at a shell thickness of 1 nm and a core radius of 5 nm. The existence of this minimum means that one way of reducing the tendency for roughening is to go to smaller core radii. By reducing R_1 from $R_1=25$ nm to $R_1 = 5$ nm, one can achieve a reduction in S_{fg} by as much as 1

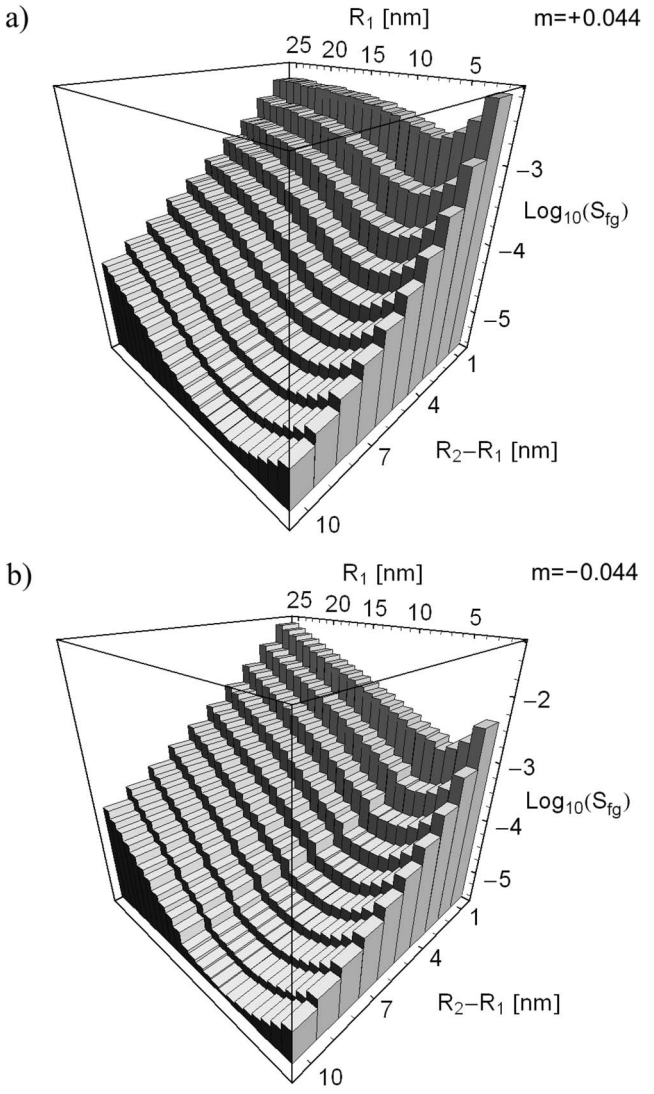

FIG. 6. $\log_{10}(S_{fg})$ as a function of the core radius R_1 and the shell thickness R_2-R_1. (a) $m=+0.044$ (Si-core-Ge shell) and (b) $m=-0.044$ (Ge-core-Si shell) using $G=46$ GPa, $\nu=0.26$, $\tau=1.0$ N m^{-1}, and $\gamma=1.5$ J m^{-2}.

order of magnitude, which means a significant increase in stability.

To see whether this minimum is also present for different values of m, and whether this is just an effect of considering surface stress, $\log_{10}(S_{fg})$ is shown in Fig. 7 for a fixed shell thickness of 1 nm as a function of the core radius R_1 and the misfit parameter m. Surface stress is neglected now. One can see in Fig. 7 that S_{fg} shows a pronounced dependence on m. A strong m dependence could be expected, since the stability critically depends on the elastic energy of the strain field, which is proportional to m^2. The minimum of S_{fg}, which could be seen in Fig. 6, is also present in Fig. 7, though only for large misfits $m \gtrsim 0.03$. Thus, one has to conclude that the existence of such a radius maximal surface stability is not just an effect of surface stress but a general feature.

One may ask whether this whole discussion on which one is the fastest growing mode does have any practical relevance. We believe it has, and to support this statement, the

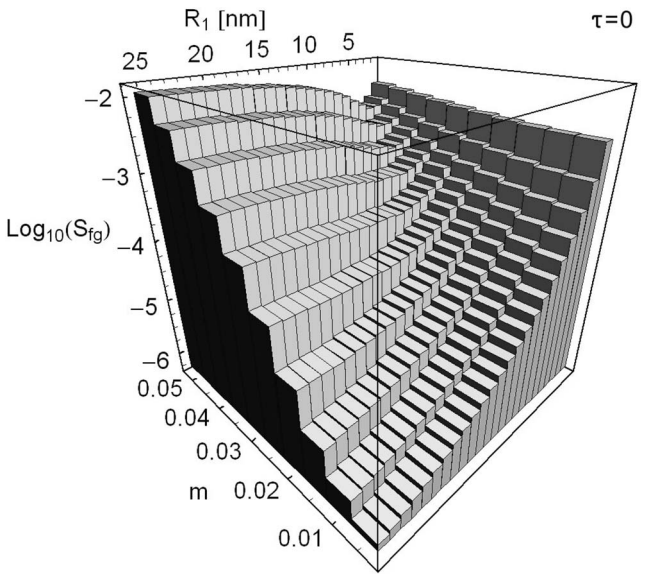

FIG. 7. $\log_{10}(S_{fg})$ as a function of the core radius R_1 and the misfit parameter m for a fixed shell thickness of 1 nm using $G=46$ GPa, $\nu=0.26$, $\tau=0$ N m^{-1}, and $\gamma=1.5$ J m^{-2}.

experimental results of Pan *et al.*[14] are reprinted in Fig. 8. One can see in their case the deposition of Ge on thick Si nanowires, with diameters in the range of about 100 nm led to the development of Ge-rich islands on the surface, with the island size being in the range of 30–50 nm. What is so interesting about these islands is that they appear to be nonrandomly distributed. Instead of a random distribution, Fig. 8 shows islands that are located in two separate rows on opposite sides of the nanowire and aligned along the axial direction. With our previous discussion in mind, it becomes clear

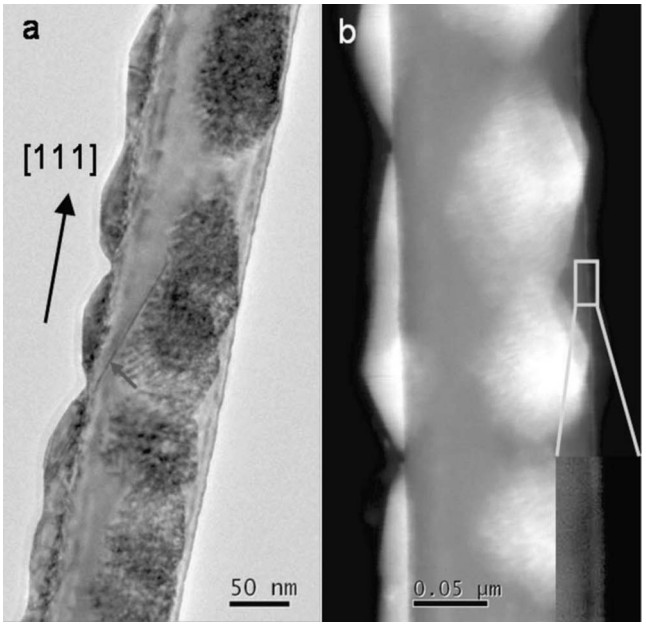

FIG. 8. (a) Bright-field transmission electron microscopy and (b) annular dark-field scanning tunneling electron microscopy images of the Ge islands deposited on Si nanowires. For more detailed information, see Ref. 14.

that such a behavior–one island on one side, one island on the opposite site–is consistent with an $n=2$ mode being the fastest growing mode.

We can compare how this experimental finding fits to the results of our calculation. We have seen in Fig. 6 that the shell is most unstable in the initial phase of growth. Thus, we assume that the actual mode of surface instability is fixed by the fastest growing mode of the initial phase of growth, e.g., at a shell thickness of 1 nm. Concerning the misfit at the interface, Pan *et al.*[14] found that the Ge content of islands is reduced to 75%–85% Ge. Supposing Si-Ge interdiffusion to be even more pronounced in the initial phase of growth, a misfit of $m=0.02$, corresponding to a shell composition of about half Si half Ge, seems to be a reasonable estimate. Here we neglect the interplay between the morphological and compositional instability.[40,41] Under these conditions—a shell thickness of 1 nm, $m=0.02$, $R_1=50$ nm, $G=46$ GPa, $\nu=0.26$, $\gamma=1.5$ J m^{-2}, and $\tau=0$ N m^{-1}—the $n=2$ mode indeed becomes the fastest growing mode. The maximum of this $n=2$ mode occurs at a wave number $q_{fg}\approx 0.07$ nm^{-1}, corresponding to a wavelength of about 90 nm, which roughly fits to the experimental results of Pan *et al.*[14] reproduced in Fig. 8. In this context, however, it must be mentioned that the outcome of the calculation, in particular regarding the question of the fastest growing mode, strongly depends on the actual choice of parameters.

To conclude, we have performed a linear stability analysis for misfit-strained core-shell nanowires considering nonaxially symmetric modes and surface stress. Within the framework of our model we could show that the surface is most unstable when the shell thickness of the order 1 nm or less. Consequently, the initial phase of growth would be most critical with respect to roughening of the surface. In addition, our model shows that for $m\gtrsim 0.03$ there exists a core radius of maximum stability, which means that it should be easiest to produce cylindrical core-shell nanowires with a core diameter of about 5–10 nm. Agreement with experimental results reported by Pan *et al.*[14] could be obtained for a certain range of parameters.

ACKNOWLEDGMENTS

This work was partially funded by BMBF project CrysGaN under Contract No. 01BU0624 and supported by the German-Israel Project No. DIP-K 6.1, the *nanoSTRESS* project, and the NODE project EU under Grant No. 015783.

APPENDIX A: LINEARIZED SURFACE DIFFERENTIAL OPERATORS AND CURVATURE

The vector $\mathbf{R}_s=R_s\hat{\mathbf{r}}+z\hat{\mathbf{z}}$, with R_s given by Eq. (1), defines the position of a point on the surface of the nanowire. Following the work of Weatherburn,[42] let us define two vectors $\mathbf{r}_1$ and $\mathbf{r}_2$,

$$\mathbf{r}_1=\frac{1}{R_s}\partial_\phi\mathbf{R_s}=\begin{pmatrix}\eta_\phi\\1\\0\end{pmatrix}, \tag{A1}$$

$$\mathbf{r}_2=\partial_z\mathbf{R_s}=\begin{pmatrix}\eta_z\\0\\1\end{pmatrix}, \tag{A2}$$

with

$$\eta_\phi=\delta\frac{n}{R_2}\cos(qz)\sin(n\phi), \tag{A3}$$

$$\eta_z=\delta q\,\sin(qz)\cos(n\phi). \tag{A4}$$

Then the outward normal of the perturbed shell surface is given by[42]

$$\tilde{\mathbf{n}}^{(2)}=H^{-1}\mathbf{r}_1\times\mathbf{r}_1=H^{-1}\begin{pmatrix}1\\\eta_\phi\\\eta_z\end{pmatrix}, \tag{A5}$$

where $H=\sqrt{1-\eta_\phi^2+\eta_z^2}$ is a normalization factor that, however, in a linear approximation becomes equal to 1. With these prerequisites, the surface gradient ∇_s can now be obtained,

$$\nabla_s=H^{-2}(\mathbf{r}_2\times\tilde{\mathbf{n}}^{(2)})\frac{1}{R_s}\partial_\phi+H^{-2}(\tilde{\mathbf{n}}^{(2)}\times\mathbf{r}_1)\partial_z$$
$$=\frac{1}{H^2}\begin{pmatrix}-\eta_\phi\\1+\eta_z^2\\-\eta_z\eta_\phi\end{pmatrix}\frac{1}{R_s}\partial_\phi+\frac{1}{H^2}\begin{pmatrix}-\eta_z\\-\eta_z\eta_\phi\\1+\eta_\phi^2\end{pmatrix}\partial_z.$$

Ignoring terms of second and higher order in δ gives the linearized surface gradient

$$\nabla_s=\begin{pmatrix}-\eta_\phi R_s^{-1}\partial_\phi-\eta_z\partial_z\\R_s^{-1}\partial_\phi\\\partial_z\end{pmatrix}. \tag{A6}$$

Using the above results the linearized surface divergence acting on the vector $\mathbf{A}=A_r\hat{\mathbf{r}}+A_\phi\hat{\boldsymbol{\phi}}+A_z\hat{\mathbf{z}}$ reads

$$\nabla_s\cdot\mathbf{A}=\left(\frac{1}{R_s}-\frac{\eta_\phi}{R_s}\partial_\phi-\eta_z\partial_z\right)A_r+\frac{1}{R_s}(\partial\phi+\eta_\phi)A_\phi+\partial_zA_z. \tag{A7}$$

The linearized surface Laplacian then becomes

$$\Delta_s=\nabla_s\cdot\nabla_s=\frac{\eta_\phi}{R_s^2}\partial_\phi+\frac{1}{R_s^2}\partial_\phi^2-\frac{\eta_z}{R_s}\partial_z+\partial_z^2. \tag{A8}$$

To zeroth order in δ this becomes equal to Eq. (67).

The curvature of the surface can most easily be obtained by calculating the divergence of the normal vector[43] using Eq. (A7) together with Eqs. (A3) and (A4).

$$\kappa=\nabla_s\cdot\tilde{\mathbf{n}}^{(2)}=\frac{1}{R_s}+\delta\left(\frac{n^2}{R_s^2}+q^2\right)\cos(qz)\cos(n\phi). \tag{A9}$$

By inserting expression (1) for R_s and using the first order expansion of $(1+x)^{-1}=(1-x)$, this finally gives

$$\kappa = \nabla_s \cdot \tilde{\mathbf{n}}^{(2)} = \frac{1}{R_2} + \delta\left(\frac{n^2-1}{R_2^2} + q^2\right)\cos(qz)\cos(n\phi). \tag{A10}$$

APPENDIX B: SURFACE BOUNDARY CONDITIONS

According to Alexander and Johnson[33] the following boundary conditions have to be applied to a liquid fluid interface at equilibrium,

$$\sigma\mathbf{n} + P^f\mathbf{n} - \nabla_s \cdot \mathbf{T} = 0, \tag{B1}$$

where $\mathbf{T}$ is the Cauchy stress tensor and P^f is the pressure in the fluid. For a solid, if the surface stress is isotropic, i.e., $\tau_{ij} = \tau\delta_{ij}$, then $\mathbf{T}$ can be expressed as a projection onto the surface[43] $\mathbf{T} = \tau(1 - \mathbf{n}\otimes\mathbf{n})$. Additionally, exploiting the fact that $\nabla_s \cdot \mathbf{n} = \kappa$ gives

$$\sigma\mathbf{n} + P^f\mathbf{n} + \tau\kappa\mathbf{n} = 0, \tag{B2}$$

which for $\mathbf{n} = \tilde{\mathbf{n}}^{(2)}$ is equivalent to Eq. (25). The solution of the first order boundary condition problem assuming equal elastic constants for core and shell can be obtained by solving the following set of equations for the unknowns d_2, f_2, and g_2:

$$0 = \delta R_2\tau(n^2 - 1 + R_2q^2) + \frac{G(n-1)R_2\nu}{1-2\nu}(6g_2 - 8g_2\nu - d_2q)\delta_{n1} - \frac{2G}{q}[8g_2(1-n)n(1-\nu) - (f_2+g_2)(3-2\nu)R_2^2q^2$$
$$- (2g_2n + d_2q)(n - n^2 - R_2^2q^2)]\mathcal{I}_n(qR_2) - 2GR_2[(f_2-g_2)n(5-4\nu) - d_2q + (f_2+g_2)(4-4\nu+n^2+R_2^2q^2)]\mathcal{I}_{n+1}(qR_2), \tag{B3}$$

$$0 = -\frac{2G\delta mnR_1^2(1+\nu)}{R_2(1-\nu)} + \frac{G(n-1)R_2}{2}(6g_2 - 8\nu g_2 - d_2q)\delta_{n1} + \frac{G}{q}\{2n(n-1)[d_2q - 2g_2(4-4\nu-n)] + 2[n(f_2+g_2)$$
$$+ 2(f_2-g_2)(1-\nu)]R_2^2q^2\}\mathcal{I}_n(qR_2) + 2GR_2[d_2qn - f_2(1+n)(4-4\nu+n) + g_2(1-n)(4-4\nu-n)]\mathcal{I}_{n+1}(qR_2), \tag{B4}$$

$$0 = -\frac{\delta q[R_2\tau(1-\nu) + 2GmR_1^2(1+\nu)]}{1-\nu} + \frac{GR_2^2q}{2}(6g_2 - 8\nu g_2 - d_2q)\delta_{n1} + 2GR_2[d_2nq - 2g_2n(2-2\nu-n)$$
$$+ (f_2+g_2)R_2^2q^2]\mathcal{I}_n(qR_2) + 2GR_2^2q[d_2q - (f_2-g_2)n + 2(f_2+g_2)(1-\nu)]\mathcal{I}_{n+1}(qR_2). \tag{B5}$$

*vschmidt@mpi-halle.de

[1] M. L. Lee, E. A. Fitzgerald, M. T. Bulsara, M. T. Currie, and A. Lochtefeld, J. Appl. Phys. **97**, 011101 (2005).
[2] L. J. Lauhon, M. S. Gudiksen, D. Wang, and C. M. Lieber, Nature (London) **420**, 57 (2002).
[3] V. Schmidt, H. Riel, S. Senz, S. Karg, W. Riess, and U. Gösele, Small **2**, 85 (2006).
[4] J. Tersoff and F. K. LeGoues, Phys. Rev. Lett. **72**, 3570 (1994).
[5] R. J. Asaro and W. A. Tiller, Metall. Trans. **3**, 1789 (1972).
[6] M. A. Grinfel'd, Sov. Phys. Dokl. **31**, 831 (1986).
[7] D. J. Srolovitz, Acta Metall. **37**, 621 (1989).
[8] H. Gao and W. D. Nix, Annu. Rev. Mater. Sci. **29**, 173 (1999).
[9] B. J. Spencer, P. W. Voorhees, and S. H. Davis, Phys. Rev. Lett. **67**, 3696 (1991).
[10] B. J. Spencer, P. W. Voorhees, and S. H. Davis, J. Appl. Phys. **73**, 4955 (1993).
[11] D. J. Kirill, S. H. Davis, M. J. Miksis, and P. W. Vorhees, Proc. R. Soc. London, Ser. A **455**, 3825 (1999).
[12] J. Colin, J. Grilhé, and N. Junqua, Philos. Mag. A **76**, 793 (1997).
[13] F. Yang and W. Song, Int. J. Solids Struct. **43**, 6767 (2006).
[14] L. Pan, K.-K. Lew, J. M. Redwing, and E. C. Dickey, Nano Lett. **5**, 1081 (2005).
[15] W. W. Mullins, J. Appl. Phys. **28**, 333 (1957).
[16] L. D. Landau and E. M. Lifshitz, *Theory of Elasticity*, Course of Theoretical Physics Vol. 7, 3rd ed. (Elsevier, Butterworth, Heinemann, Oxford, 1986), Chap. 1, pp. 1–36.
[17] J. W. Gibbs, *The Scientific Papers of J. Williard Gibbs, Ph.D., LL. D.*, Thermodynamics Vol. I (Longmans, Green, London, 1906), Chap. 3, pp. 315–318.
[18] R. Shuttleworth, Proc. Phys. Soc., London, Sect. A **63**, 444 (1950).
[19] J. W. Cahn, Acta Metall. **28**, 1333 (1980).
[20] O. L. Alerhand, D. Vanderbilt, R. D. Meade, and J. D. Joannopoulos, Phys. Rev. Lett. **61**, 1973 (1988).
[21] M. T. Middel, H. J. W. Zandvliet, and B. Poelsema, Phys. Rev. Lett. **88**, 196105 (2002).
[22] J. J. Métois, A. Saúl, and P. Müller, Nat. Mater. **4**, 238 (2005).
[23] M. C. Payne, N. Roberts, R. J. Needs, M. Needels, and J. D. Joannopoulos, Surf. Sci. **211-212**, 1 (1989).
[24] R. D. Meade and D. Vanderbilt, Phys. Rev. Lett. **63**, 1404 (1989a).
[25] H. Sato and K. Yagi, J. Phys.: Condens. Matter **5**, 2095 (1993).
[26] R. D. Twesten and J. M. Gibson, Phys. Rev. B **50**, 17628 (1994).

[27] R. D. Meade and D. Vanderbilt, Phys. Rev. B **40**, 3905 (1989).
[28] J. van Heys and E. Pehlke, Phys. Rev. B **72**, 125351 (2005).
[29] J. J. Wortman and R. A. Evans, J. Appl. Phys. **36**, 153 (1965).
[30] P. F. Papkovich, Izv. Akad. Nauk SSR Ser. Fiz. Mat. Nauk **10**, 1425 (1932).
[31] H. Neuber, Z. Angew. Math. Mech. **14**, 203 (1934).
[32] M. H. Sadd, *Elasticity: Theory, Applications and Numerics* (Elsevier, New York, 2005), Chap. 13, pp. 347–358.
[33] J. I. D. Alexander and W. C. Johnson, J. Appl. Phys. **58**, 816 (1985).
[34] F. C. Larché and J. W. Cahn, Acta Metall. **33**, 331 (1985).
[35] P. H. Leo and R. F. Sekerka, Acta Metall. **37**, 3119 (1989).
[36] R. J. Jaccodine, J. Electrochem. Soc. **110**, 524 (1963).
[37] J.-M. Zhang, F. Ma, K.-W. Xu, and X.-T. Xin, Surf. Interface Anal. **35**, 805 (2003).
[38] M. T. Plateau, Philos. Mag. **12**, 286 (1856).
[39] L. Rayleigh, Proc. London Math. Soc. **s1-10**, 4 (1878).
[40] F. Glas, Phys. Rev. B **55**, 11277 (1997).
[41] B. J. Spencer, P. W. Voorhees, and J. Tersoff, Phys. Rev. B **64**, 235318 (2001).
[42] C. E. Weatherburn, Compos. Math. **4**, 342 (1937).
[43] T. V. Savina, P. W. Voorhees, and S. H. Davis, J. Appl. Phys. **96**, 3127 (2004).